

OPTIMIZATION OF LOW-ENERGY BEAM TRANSPORT *

H.R. Kremers, J.P.M. Beijers, and S. Brandenburg
KVI-CART, Groningen, The Netherlands

Abstract

Transport of low-energy heavy-ion beams from an Electron Cyclotron Resonance Ion Source to an accelerator often suffers from significant emittance increase caused by aberrations of ion-optical elements in the beam transport line. In this paper we use a combination of four-dimensional phase-space measurements and simulations to study beam transport through an analyzing magnet. It is shown that large second-order aberrations of the magnet lead to a five-fold increase of the beam emittance. Several mitigation strategies are investigated, i.e. adding compensating hexapoles or extra focusing elements between ion source and magnet. The best solution is to use a focusing solenoid between ion source and magnet. Using a compensating hexapole is not recommended, since it introduces significant third and higher-order aberrations.

INTRODUCTION

Low-energy heavy-ion beams extracted from Electron Cyclotron Resonance Ion Sources (ECRIS) have relatively large beam diameters and divergences because the extraction occurs in a decreasing magnetic field. Such beams are therefore very sensitive for ion-optical aberrations in the bending and focusing elements of the beam transport line leading to emittance blowup and beam losses. To give some typical numbers¹, injector ECRIS's have beam emittances in the range of 20-100 mm mrad for low to medium charged ions. The geometrical acceptance of a cyclotron is typically 100-200 mm mrad. However, measured emittances in low-energy beam lines are often in the range of 100-300 mm mrad taking into account the phase space cut-offs by beam limiters. This results in low transport and injection efficiencies [2–4]. There is thus much room for improvement. These issues are particularly relevant for very high-intensity beams where beam losses might lead to damage, or for very low-intensity beams where one cannot afford to lose any ions.

This paper presents methods to determine the beam emittance and ion-optical aberrations quantitatively and discusses possible ways to minimize the emittance blowup caused by these aberrations. The motivation for this work was to better understand beam transport in the low-energy beam transport (LEBT) line of the AGOR facility at KVI-CART [5, 6]. The measurements and simulations have been done with a mono-component 25 keV He⁺ beam only for the first part of this LEBT line consisting of an ECRIS and a charge-state analyzing magnet, but it is straightforward to

include more ion-optical elements. Regarding the simulations to minimize the ion-optical aberrations of the dipole magnet a 21 keV H⁺ beam is used. The paper is organized in three sections. The first section describes the experimental and computational methods that have been used. The second section presents and discusses several ways to minimize ion-optical aberrations. The last section finishes with the conclusions.

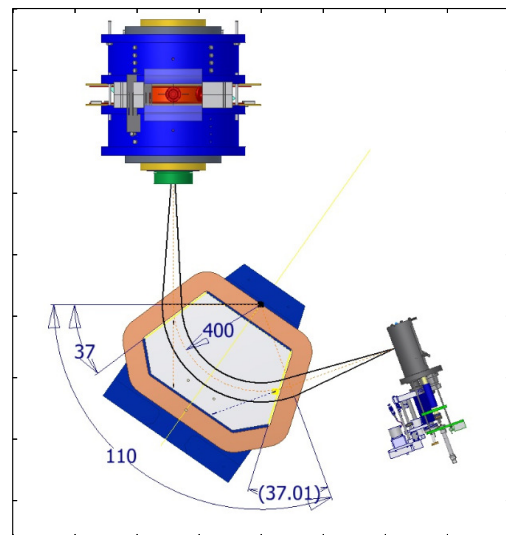


Figure 1: ECR ion source, charge-state analyzing magnet and a pepper-pot emittance meter.

EXPERIMENTAL AND COMPUTATIONAL METHODS

Experimental setup

The first part of the LEBT line includes an ECRIS, charge-state analyzing magnet and a pepper-pot emittance meter (see Fig. 1). The ECRIS is of the AECR-type with two room temperature solenoids and an open NdFeB permanent hexapole magnet. The plasma is heated with 14 GHz microwaves with a maximum power of 2 kW and the source can be biased with respect to ground up to a maximum voltage of 34 kV. Ions are extracted with an accel-decel lens system consisting of a plasma electrode with a 8 mm extraction aperture followed by shielding and ground electrodes. Charge-state selection of the extracted beam is done with an unclamped double-focusing analyzing magnet with a bending radius of 400 mm, bending angle of 110° and pole face

* Work supported by university of Groningen (RuG).

¹ All quoted beam emittances are understood to be 4-rms emittances according to the definition of Lapostolle [1].

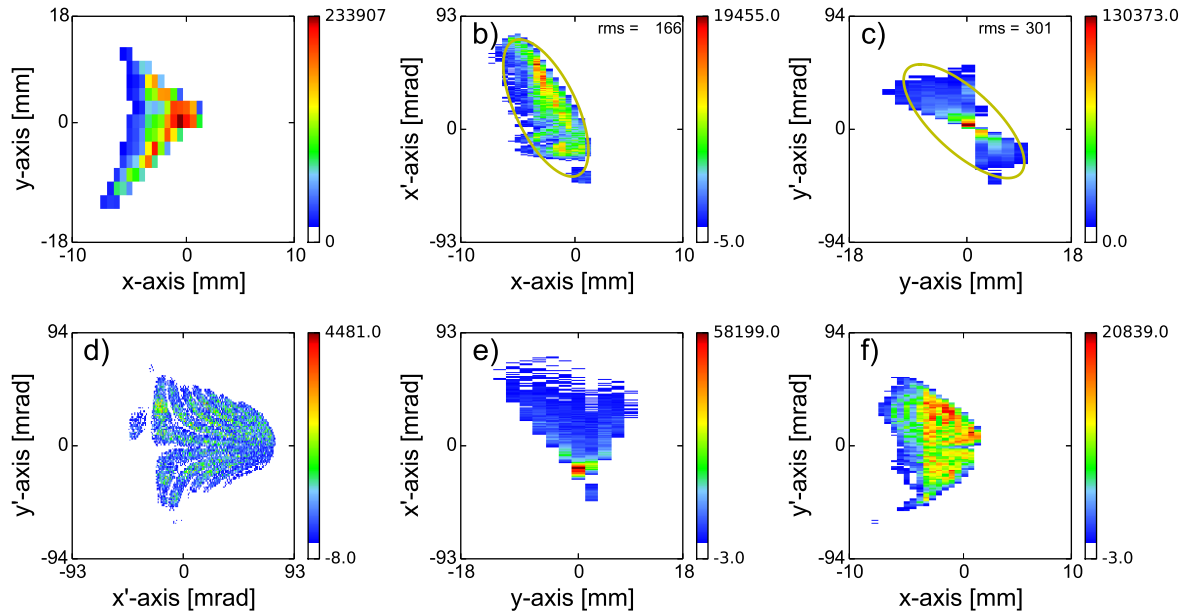


Figure 2: Measured six 2D projections validated by simulations of the 4D phase-space distribution of a 25 keV He⁺ beam.

rotations of 37°. The geometrical acceptance of the magnet is 60 mm in both horizontal and vertical directions. The distance between the plasma electrode and effective field boundary (EFB) of the magnet is 682 mm.

In order to benchmark the beam transport simulations we have installed a pepper-pot emittance meter close to the image plane of the analyzing magnet [7]. The advantage of a pepper-pot emittance meter compared to a scanning-slit device is that with a pepper-pot meter one can measure the full four-dimensional (4D) transverse phase-space distribution of ion beams including correlations between the horizontal and vertical planes, while a scanning-slit meter only measures the $(x-x')$ and the $(y-y')$ projections of the 4D distribution. Figure 2 shows six 2D projections of the 4D phase-space distribution of a 25 keV He⁺ beam measured with the pepper-pot emittance meter. Notice the large horizontal and vertical emittances of 116 and 301 mm mrad, respectively, and the higher-order horizontal and vertical correlations in the extracted ion beam. These values would even be a factor of two larger without the beam losses caused by the geometrical acceptance of the system.

Computational methods

We have used several codes to simulate and analyze the extraction and transport of low-energy heavy-ion beams, which are all based on numerically calculating ion trajectories in predefined electromagnetic fields. In previous work we have simulated the ion production in an ECRIS using a Particle-In-Cell, Monte-Carlo-Collision (PIC-MCC) code with which the phase-space distribution of the ions in the extraction aperture of the plasma electrode has been calculated [8]. The ion trajectories through the accel-decel

extraction system, drift spaces and analyzing magnet have been calculated with the General Particle Tracer (GPT) code, which is a 3D particle tracking code taking all electric and magnetic fields in the extraction system and analyzing magnet into account as well as the space-charge forces of the ion beam [9]. The LORENTZ-3D code has mainly been used to calculate the 3D magnetic field of the analyzing magnet [10]. These simulations, confirmed by measurements, showed that i) ion beams are fully space-charge neutralized so that the Coulomb forces between ions can be neglected, ii) the ion beam behind the extraction system is strongly divergent, has a triangular spatial profile and 4rms-emittances of 65 mm mrad in both transverse directions determined by the fringe field of the extraction solenoid and iii) large, second-order aberrations of the analyzing magnet cause a five-fold increase of the beam emittances in the magnet's image plane [11].

To further investigate the emittance increase in the analyzing magnet and possible ways to remedy this we use COSY INFINITY [12]. This code applies differential-algebra methods to calculate transfer maps of ion-optical systems up to an arbitrary order. In the present work we have calculated transfer maps of the analyzing magnet and additional focusing elements up to 5th order. An axisymmetric Kapchinsky-Vladimirski (KV) distribution with an emittances of $\epsilon_{4rms} = 65$ mm mrad in both transverse planes is used as an initial phase-space distribution. We use this distribution because previous simulations showed that the emittance of the extracted beams are elliptical and nearly identical in both transversal directions [11]. KV distributions have a uniform intensity and are completely contained in an ellipse with an area of $\epsilon_{4rms}\pi$ mm mrad. The

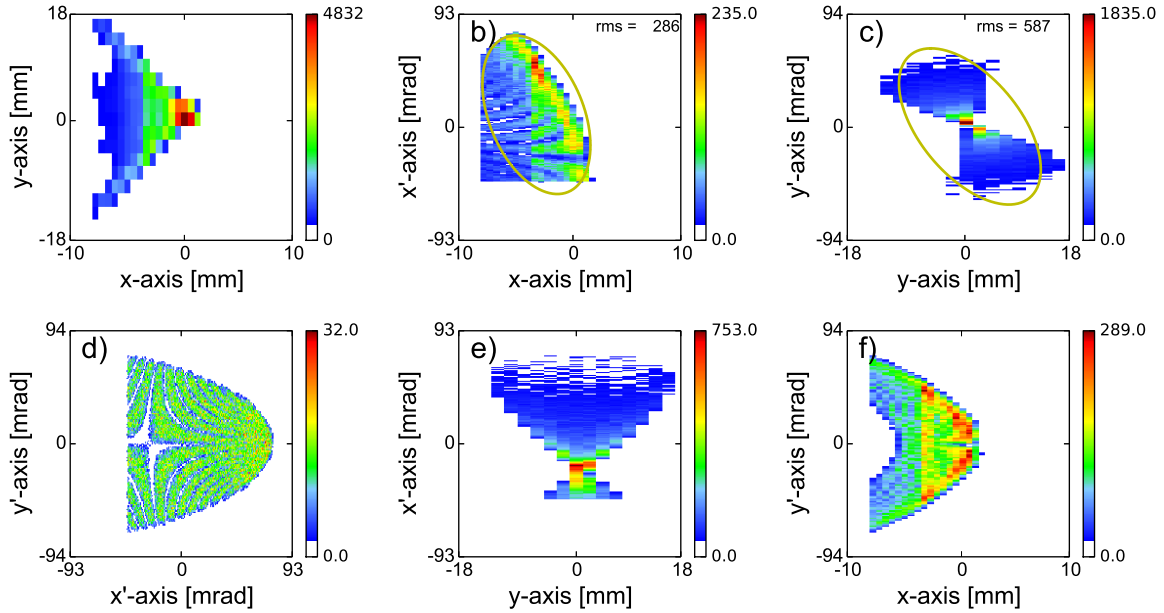


Figure 3: Calculated six 2D projections of the 4D phase-space distribution of a 25 keV He⁺ beam. Phase-space cutoffs caused by finite apertures of the magnet have been taken into account.

initial KV distribution $f^0(x, x', y, y')$ is then transformed to a final distribution $f^1(x, x', y, y')$ by randomly sampling f^0 with 10^8 particles, i.e. the transformed phase-space coordinates q_1 in the image plane of the analyzing magnet are related to the initial coordinates q_0 in the object plane by $q_1 = M^{(k)} q_0$ with $M^{(k)}$ the transfer map of the system of order k and $q = x, x', y, y'$. To illustrate, Figure 3 shows six 2D projections of a calculated 4D phase-space distribution of a 25 keV He⁺ beam using a second-order transfer map of the analyzing magnet. We used an internal model (FR3) of COSY INFINITY to calculate the fringe fields of the analyzing magnet. Phase-space cutoffs caused by finite apertures of the magnet have been taken into account. The measured and calculated phase-space distributions show good agreement and we conclude that the second order coefficients $(y|x'y')$, $(x|y'y')$ and $(x|x'x')$ are the dominant terms causing a five-fold increase of the beam emittance behind the analyzing magnet.

MINIMIZING ION-OPTICAL ABERRATIONS

Two strategies have been studied to minimize the second order aberrations. The first strategy is to compensate the second order terms with two hexapoles, one before and one behind the analyzing magnet. The second strategy is to use a "field lens" in front of the analyzing magnet to modify the divergent extracted beam into a more parallel beam. In this way the influence of the strong gradients of the fringe field of the dipole is reduced. We consider both a solenoid and an einzel lens.

Hexapole lenses

The hexapoles are positioned at the entrance and exit of the dipole magnet at a distance of 305 and 152 mm of the magnet respectively. The effective length of the hexapoles is 100 mm and the distance between the beam axis and the pole tip is 50 mm. The hexapoles reduce the 2nd order coefficients $(y|x'y')$ and $(x|y'y')$ to nearly zero, but the coefficient $(x|x'x')$ is increased by a factor of 3. That hexapoles are not able to compensate fully for all three coefficients is due to fact that they generates the coefficients: $(y|x'y')$, $(x|x'x')$ and $(x|y'y')$ in a ratio of 1 : +0.5 : -0.5. As the second order coefficients of the magnet aberration do not exhibit these exact ratios the term $(x|x'x')$ remains. Furthermore, third and higher order coefficients become significant in both planes. In Fig. 4 the value of the 4-rms emittance is shown as function of the poletip field of the hexapole. Notice that the minimum value of the horizontal and vertical emittances is reached at different poletip fields.

Field lenses

A thin solenoid with an inner diameter of 200 mm is positioned 305 mm upstream from the dipole magnet. The solenoid reduces the three second order coefficients $(y|x'y')$, $(x|y'y')$ and $(x|x'x')$ to nearly zero. When the solenoid is powered with a current of 320 kA, turn the wide divergent H⁺ beam, at the entrance of the dipole magnet, is changed into a smaller more paraxial beam. In this way the beam fits in a more effective way the geometrical acceptance of the magnet and the influence of the strong gradients of the fringe field of the dipole is reduced. This effect is significant as can be seen in Fig. 5. The value of 74 mm mrad

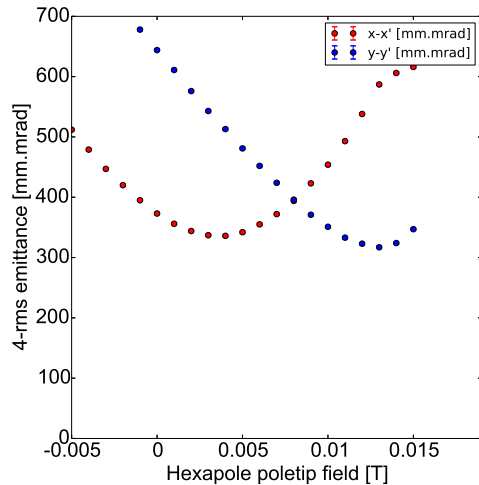


Figure 4: Calculated 4-rms emittance value of a 21 keV H^+ beam in the image plane of the dipole magnet as function of the excitation of the hexapoles.

for the 4-rms emittance at 320 kA.turn is of the same order as the 4rms emittance of the initial KV distribution in the object plane. Including a solenoid in the extraction area with this strength is difficult as the magnetic field of the solenoid interferes with the fringe field in the extraction region of the ion source. Therefore, we investigated also a simpler and smaller option i.e an einzel lens.

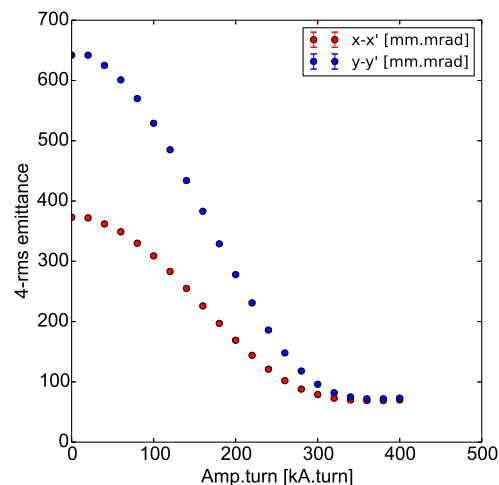


Figure 5: Calculated 4-rms emittance value of a 21 keV H^+ beam in the image plane of the dipole magnet as function of the excitation of the solenoid.

An Einzel lens reduces the coefficients $(y|x'y')$, $(x|y'y')$ and $(x|x'x')$ of the second-order transfer map by a factor of 4 by modifying the divergent beam into a more paraxial beam in both transverse directions. Quantitatively, the 4-rms emittance is changed from 375 mm mrad and 650 mm mrad in the horizontal and vertical plane to 120 and

140 mm mrad, respectively. The einzel lens has three identical cylinders, each with an inner diameter of 70 mm and a length of 75 mm. The gap between the cylinders is 10 mm. The distance between the lens and the dipole magnet is 305 mm. As shown in the Fig. 6 a minimum is found for the emit-

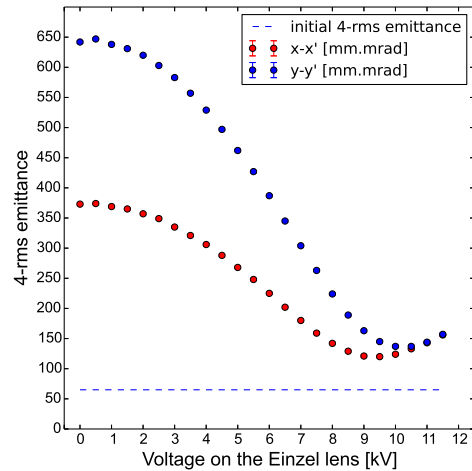


Figure 6: Calculated 4-rms emittance value of a 21 keV H^+ beam in the image plane of the dipole magnet as function of the potential on the einzel lens.

tances in both transverse directions at a lens-potential of 9-10 kV. However the initial 4rms-emittance of 65 mm mrad is not regained. A detailed investigation shows that this is caused by the additional aberrations induced by the einzel lens itself. Simulations are in progress for an accel-decel configuration since the aberrations of such a configuration are expected to be smaller with respect to the decel-accel configuration.”

CONCLUSIONS

By comparing 4D phase-space measurements and simulations we have identified large second-order aberrations of the analyzing magnet as the main cause of emittance blowup and beam loss in the LEBT line connecting the ECRIS and AGOR cyclotron. The large second-order aberrations are mainly caused by the large divergences that are characteristic of ECRIS beams. Several mitigation strategies have been studied, including compensating hexapoles and a focusing solenoid or einzel lens between ECRIS and analyzing magnet. Our simulations show that adding hexapoles can indeed compensate the second-order aberrations to a large extent, but introduce additional third and higher-order aberrations. Clearly the best solution is a focusing solenoid, with a large inner diameter, between ECRIS and analyzing magnet which, if it has enough focusing power, can recover the initial emittances before the analyzing magnet. When a solenoid cannot be used, e.g. because of space limitations, using an einzel lens is the second best option. However, enough care should be exercised in its design as not to introduce additional aberrations.

In general, efficient transport of low-energy ECRIS beams with minimal losses can be realized by keeping the beam as paraxial as possible and paying sufficient attention to minimize the fringe fields of the bending and focusing elements. Although this remark may sound superficial it is often overlooked by designers of LEBT lines, who tend to design optical elements which are too short with too small apertures and thus have relatively large fringe fields.

REFERENCES

- [1] P.M. Lapostolle, IEEE Trans. Nucl. Sci. **18**, 1101 (1971).
- [2] W. Krauss-Vogt, H. Beuscher, H. L. Hagedoorn, J. Reich and P. Wucherer, Nucl. Instrum. Methods A **268**, 5 (1988).
- [3] Cao, Y. and Zhao, H. W. and Ma, L. and Zhang, Z. M. and Sun, L. T., Rev. Sci. Instrum. **75**, 1443-1445 (2004), DOI:<http://dx.doi.org/10.1063/1.1690482>
- [4] Harrison, K. A. and Antaya, T. A., Rev. Sci. Instrum., **65**, 1138-1140 (1994), DOI:<http://dx.doi.org/10.1063/1.1145039>
- [5] H.R. Kremers et al., Rev. Sci. Instrum. **77**, 03A311 (2006).
- [6] H.R. Kremers, J.P.M. Beijers, S. Brandenburg and J. Mulder, High Energy Physics and Nuclear Physics, Vol 31, supp 1, pg 90, (2007).
- [7] H.R. Kremers, J.P.M. Beijers, and S. Brandenburg, Rev. Sci. Instrum. **84**, 025117 (2013).
- [8] V. Mironov and J.P.M. Beijers, Phys. Rev. ST Accel. Beams **12**, 073501 (2009).
- [9] General Particle Tracer code, see <http://www.pulsar.nl/gpt>
- [10] LORENTZ-3D code, see <http://www.integratedsoft.com/products/lorentz>
- [11] S. Saminathan et al., Rev. Sci. Instrum. **83**, 073305 (2012).
- [12] K. Makino and M. Bertz, Nucl. Instrum. Methods A **558**, 346